Phytochemistry 69 (2008) 3043–3053

Contents lists available at ScienceDirect

Phytochemistry

journal homepage: www.elsevier.com/locate/phytochem

Pyrone polyketides synthesized by a type III polyketide synthase from *Drosophyllum lusitanicum*

Aphacha Jindaprasert [a,b,c], Karin Springob [c,d,*], Jürgen Schmidt [c], Wanchai De-Eknamkul [b], Toni M. Kutchan [c,d]

[a] *Faculty of Agroindustry, King Mongkut's Institute of Technology Ladkrabang, Bangkok 10520, Thailand*
[b] *Department of Pharmacognosy, Faculty of Pharmaceutical Sciences, Chulalongkorn University, Bangkok 10330, Thailand*
[c] *Leibniz-Institut für Pflanzenbiochemie, Weinberg 3, 06120 Halle, Saale, Germany*
[d] *Donald Danforth Plant Science Center, 975 North Warson Road, St. Louis, MO 63132, USA*

ARTICLE INFO

Article history:
Received 19 March 2007
Received in revised form 11 February 2008
Available online 6 May 2008

Keywords:
Drosophyllum lusitanicum link
Drosophyllaceae
Naphthoquinone
Hexaketide synthase
Pyrone synthase
Type III polyketide synthase

ABSTRACT

To isolate cDNAs involved in the biosynthesis of acetate-derived naphthoquinones in *Drosophyllum lusitanicum*, an expressed sequence tag analysis was performed. RNA from callus cultures was used to create a cDNA library from which 2004 expressed sequence tags were generated. One cDNA with similarity to known type III polyketide synthases was isolated as full-length sequence and termed DluHKS. The translated polypeptide sequence of DluHKS showed 51–67% identity with other plant type III PKSs. Recombinant DluHKS expressed in *Escherichia coli* accepted acetyl-coenzyme A (CoA) as starter and carried out sequential decarboxylative condensations with malonyl-CoA yielding α-pyrones from three to six acetate units. However, naphthalenes, the expected products, were not isolated. Since the main compound produced by DluHKS is a hexaketide α-pyrone, and the naphthoquinones in *D. lusitanicum* are composed of six acetate units, we propose that the enzyme provides the backbone of these secondary metabolites. An involvement of accessory proteins in this biosynthetic pathway is discussed.

1. Introduction

Drosophyllum lusitanicum Link, the dewy pine, is a carnivorous plant that occurs in the southern part of the Iberian peninsula and northern Morocco. Taxonomically, *D. lusitanicum* belongs to the monotypic family Drosophyllaceae, as shown by recent molecular studies, but is closely related to other families with carnivorous plants, e.g the Droseraceae, Nepenthaceae and Dioncophyllaceae (Meimberg et al., 2000; Heubl et al., 2006). A chemotaxonomic marker of these taxa and related families without carnivory, e.g. the Plumbaginaceae, is the occurrence of acetogenic naphthoquinones. These secondary metabolites serve as defense compounds (Peters et al., 1995; Bringmann et al., 1999) and as antifeedants against insects (Tokunaga et al., 2004a,b), but some have allelopathic effects, as well (Dornbos and Spencer, 1990; Higa et al., 1998). Naphthoquinones are also known to possess useful pharmacological activities. Plumbagin **(8)** (2-methyl-5-hydroxy-1,4-naphthoquinone), for example, was shown to have antimicrobial (Durga et al., 1990; Didry et al., 1994), antimalarial (Likhitwitayawuid et al., 1998), and anticancer (Sugie et al., 1998; Sandur et al., 2006) effects.

The biosynthesis of naphthoquinones can occur *via* three different routes in higher plants. They can be produced from geranylated *p*-hydroxybenzoic acid, as in the case of alkannin and shikonin (Schmid and Zenk, 1971; Inouye et al., 1979), or from *iso*-chorismic acid and α-ketoglutaric acid *via* *o*-succinylbenzoic acid, providing the precursor of vitamin K (Leistner, 1999). A third pathway leading to the naphthoquinones plumbagin **(8)**, droserone and 7-methyljuglone utilizes acetate precursors. First evidence of this pathway had been provided by tracer studies with *Plumbago europaea*, *Drosera* species and *Drosophyllum lusitanicum* (Durand and Zenk, 1971,1974). Recent experiments by Bringmann and co-workers confirmed the acetogenic origin of naphthoquinones in lianas of the Ancistrocladaceae and Dioncophyllaceae families (Bringmann et al., 2000). Based on these experiments, it was postulated that plumbagin **(8)** and biosynthetically related naphthoquinones and tetralones are synthesized by polyketide synthases (PKSs) *via* the acetate-polymalonate pathway (Bringmann and Feineis, 2001).

All PKSs so far isolated from plants belong to the superfamily of type III PKSs (Schröder, 2000; Austin and Noel, 2003), which comprises homodimeric proteins that catalyze the iterative decarboxylative condensation of a starter coenzyme A (CoA) ester with malonyl-CoA **(1)**, or in some cases, methylmalonyl-CoA or ethylmalonyl-CoA (Schröder et al., 1998; Song et al., 2006). The best

* Corresponding author. Address: Donald Danforth Plant Science Center, 975 North Warson Road, St. Louis, MO 63132, USA. Tel.: +1 314 587 1490; fax: +1 314 587 1590.
E-mail address: kspringob@danforthcenter.org (K. Springob).

0031-9422/$ - see front matter © 2008 Elsevier Ltd. All rights reserved.
doi:10.1016/j.phytochem.2008.03.013

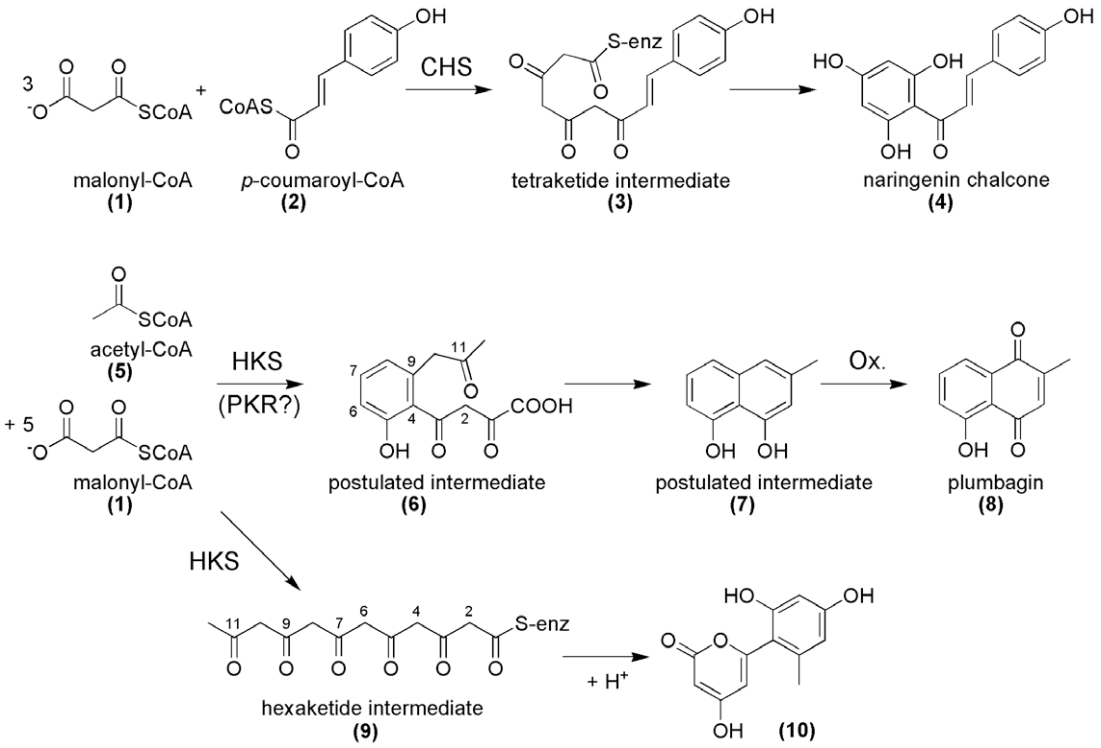

Fig. 1. Postulated mechanism of plumbagin biosynthesis and comparison with the reaction of chalcone synthase (CHS). The PKS involved in plumbagin **(8)** biosynthesis presumably catalyzes the decarboxylative condensation of acetyl-CoA **(5)** with five molecules of malonyl-CoA **(1)**. The oxygen of the third acetate unit is probably removed by a polyketide reductase (PKR) prior to the first cyclization, and one carbon is lost by decarboxylation.

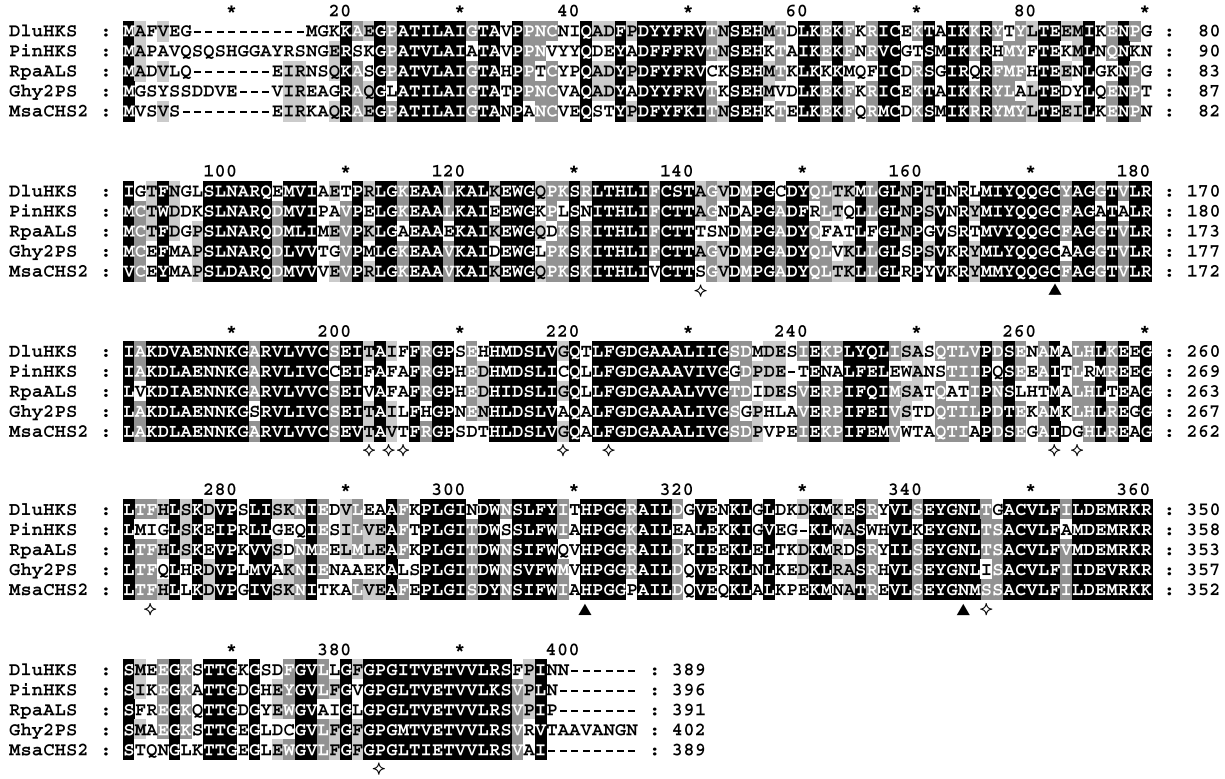

Fig. 2. ClustalW alignment of DluHKS with other type III PKS amino acid sequences. Amino acids of the catalytic Cys-His-Asn triad are marked by triangles. Other amino acids of the active site cavity, which are discussed in the text, are labeled by diamonds. Abbreviations: DluHKS, *Drosophyllum lusitanicum* HKS; Ghy2PS, *Gerbera hybrida* 2-pyrone synthase; MsaCHS2, *Medicago sativa* CHS2; PinHKS, *Plumbago indica* HKS; RpaALS, *Rheum palmatum* aloesone synthase.

studied member of this family, chalcone synthase (CHS), is a type III PKS that occurs ubiquitously in higher plants and catalyzes the pivotal step of flavonoid biosynthesis by condensing a *p*-coumaroyl-CoA **(2)** starter with three molecules of malonyl-CoA **(1)** (Fig. 1). The enzyme-linked intermediate tetraketide **(3)** subsequently undergoes an intramolecular Claisen condensation and aromatization to yield naringenin chalcone **(4)**. Apart from this prominent example, more than 20 functionally distinct type III PKSs from plants, fungi, and bacteria are known that produce a large variety of natural products. This is achieved by variation of starter and extender CoA esters, one to seven elongation steps with malonyl-CoA **(1)** and different types of cyclization. Analysis of several type III PKSs by X-ray diffraction and subsequent mutagenesis studies provided evidence that substrate selectivity and chain length depend mainly on the size and the shape of the active site cavity (Ferrer et al., 1999; Jez et al., 2000a; Sankaranarayanan et al., 2004). Many type III PKSs exhibit promiscuous substrate specificities and accept a wide range of non-physiological substrates *in vitro* (e.g. Abe et al., 2000, 2004a; Morita et al., 2000; Samappito et al., 2002, 2003). In this case, however, mainly pyrone-type derailment products are formed, most probably due to steric and/or electronic perturbations in the active site followed by release of the uncyclized polyketide from the enzyme and spontaneous lactonization (Morita et al., 2000).

The PKS involved in plumbagin **(8)** biosynthesis has to catalyze the condensation of six acetate units derived from acetyl-CoA **(5)** and malonyl-CoA **(1)**. The postulated intermediate hexaketide undergoes two aldol cyclizations and is probably modified by a ketoreductase (Fig. 1).

A recombinant type III hexaketide synthase of *Plumbago indica*, PinHKS, recently characterized by our group, catalyzes the formation of α-pyrones from three to six acetate units (Springob et al., 2007). Although the enzyme was able to condense six acetate units, plumbagin **(8)** or a naphthalene derivative were not formed, and it could not be unambiguously proven that the PKS is involved in naphthoquinone biosynthesis *in planta*. In this paper, we report the isolation of a similar cDNA from *D. lusitanicum* callus cultures by EST sequencing termed DluHKS. The biochemical characterization of the recombinant PKS provides additional evidence for the involvement of hexaketide synthases in naphthoquinone biosynthesis.

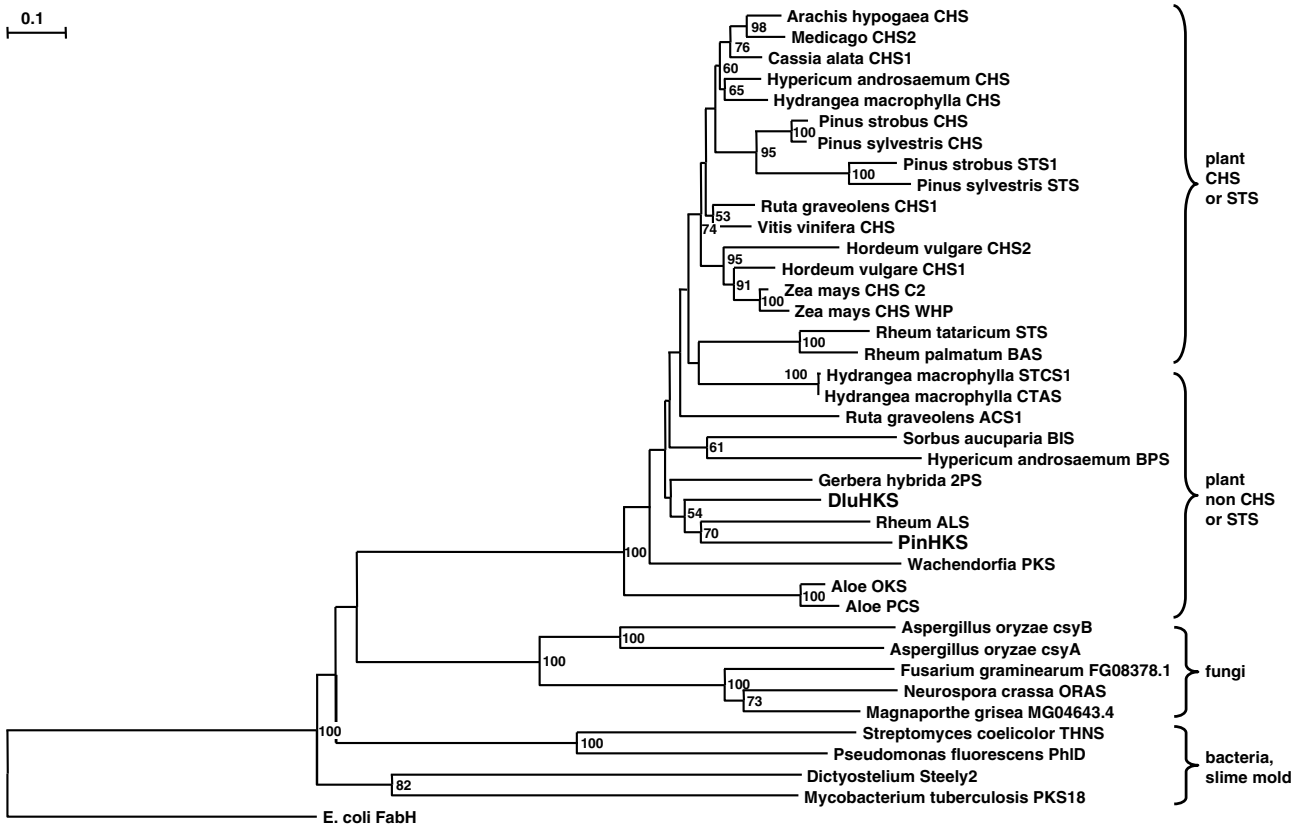

Fig. 3. Relationship of DluHKS with other type III PKSs. The tree was constructed with protein sequences of type III PKSs from plants, fungi, bacteria and one slime mold PKS (Steely 2). Except for ORAS of *Neurospora crassa*, the type III PKSs from fungi are not yet functionally characterized. *E. coli* β-ketoacyl synthase III (FabH) was used as outgroup. The phylogenetic tree was calculated using TREECON (Van de Peer and De Wachter, 1994). Construction of the tree was performed using the Neighbour-Joining algorithm, and bootstrap values higher than 50 are shown. *Abbreviations*: 2PS, 2-pyrone synthase; ACS, acridone synthase; ALS, aloesone synthase; BAS, benzalacetone synthase; BIS, biphenyl synthase; BPS, benzophenone synthase; CHS, chalcone synthase; CTAS; *p*-coumaroyl triacetic acid lactone synthase; HKS, hexaketide synthase; OKS, octaketide synthase; ORAS, 2′-oxoalkylresorcylic acid synthase; PCS, pentaketide chromone synthase; STCS, stilbenecarboxylate synthase; STS, stilbene synthase; THNS, 1,3,6,8-tetrahydroxynaphthalene synthase. GenBank accession numbers: *Aloe arborescens* OKS (AAT48709) and PCS (AAX35541), *Aspergillus oryzae* csyA (BAD97390) and csyB (BAD97391), *Arachis hypogaea* CHS (AAO32821), *Cassia alata* CHS1 (AAM00230), *Dictyostelium dioscoideum* Steely2 (XP635518), *E. coli* FabH (1EBLB), *Fusarium graminearum* FG08378.1 (XM388554), *Gerbera hybrida* 2-PS (P48391), *Hordeum vulgare* CHS1 (CAA41250) and CHS2 (CAA70435), *Hydrangea macrophylla* CHS (BAA32732), CTAS (BAA32733), and STCS1 (AAN76182), *Hypericum androsaemum* CHS (AAG30295) and BPS (AAL79808), *Magnaporthe grisea* MG04643.4 (XM362198), *Medicago sativa* CHS2 (P30074), *Mycobacterium tuberculosis* PKS18 (AAK45681), *Neurospora crassa* ORAS (XP960427), *Pinus strobus* CHS (CAA06077) and STS1 (CAA87012), *Pinus sylvestris* CHS (CAA43166) and STS (AAB24341), *Plumbago indica* HKS (AB259100), *Pseudomonas fluorescens* PhlD (AAB48106), *Rheum palmatum* ALS (AAS87170) and BAS (AAK82824), *Rheum tataricum* STS (AAP13782), *Ruta graveolens* ACS1 (S60241) and CHS1 (Q9FSB9), *Sorbus aucuparia* BIS (ABB89212), *Streptomyces coelicolor* THNS (NP625495), *Vitis vinifera* CHS (BAA31259), *Wachendorfia thyrsiflora* PKS (AAY51378), *Zea mays* CHS C2 (AAW56964) and CHS WHP (CAA42763).

2. Results and discussion

To isolate the cDNAs encoding the naphthoquinone biosynthetic enzymes, an expressed sequence tag (EST) analysis was performed. A cDNA library was constructed with 2.5 μg Poly(A)$^+$ RNA isolated from *D. lusitanicum* calluses that have been shown to produce plumbagin **(8)** and drosophylloside, a naphthalenecarboxylic acid glucoside (unpublished results). 2004 ESTs were obtained by 5'-sequencing of randomly chosen cDNA clones, and cluster analysis yielded 1579 unigenes.

Two ESTs, W36 and Z25, showed sequence homology to known chalcone synthase (CHS) superfamily members. Isolation of the full-length clones was carried out by RACE PCR. The full-length cDNA of clone W36 could be isolated successfully by 5' RACE PCR, whereas the recovery of the missing 5' and 3' ends of Z25 was only partially successful yielding a 630 bp cDNA fragment. However, the Z25 translated polypeptide showed 93% identity and 99% similarity with W36, suggesting that the two sequences encode proteins with similar properties. Hence, only W36 was chosen for further analysis and termed DluHKS. The full-length cDNA sequence of DluHKS was 1442 bp containing a 133 bp 5'-non-coding region, a 1170 bp open reading frame (ORF) with start- and stop-codons encoding a protein with 389 amino acid residues and a 139 bp 3'-non-coding region. The predicted molecular weight of the encoded protein is 42.8 kDa.

The nucleotide sequence of DluHKS will appear in the DDBJ/EMBL/GenBank databases with the accession number EF405822. The translated polypeptide sequence of DluHKS showed 51–67% identity with plant type III PKSs and ca. 20% identity with bacterial type III PKSs. Highest identities (69%) were found with a CHS of *Vitis vinifera*, while the identity to *P. indica* HKS (PinHKS), which has been proposed to be involved in naphthoquinone formation, was only 58%. DluHKS contains the conserved Cys-His-Asn catalytic triad-like other type III PKSs (Fig. 2). In addition, several residues that are important for the active-site geometry and for the steric modulation of enzyme activity are conserved between DluHKS and CHS, e.g. Gly211, Phe215, Phe265 and Pro375 (numbering according to *Medicago sativa* CHS2) (Ferrer et al., 1999; Austin and Noel, 2003). However, in comparison with *M. sativa* CHS2, the sterically important active site positions Ser133, Thr197, Gly256 and Ser338 are changed to Ala, Phe, Leu and Thr, respectively. Most of these exchanges are also found in the sequence of PinHKS, except for the residue at position 197, which is Ala in PinHKS (Fig. 2).

A phylogenetic analysis was performed with plant, bacterial, fungal and slime mold type III PKSs using *Escherichia coli* (*E. coli*) β-ketoacyl synthase III as outgroup (Fig. 3). In the tree, plant PKSs form a distinct cluster, and CHSs and most stilbene synthases (STSs) group separately from plant PKSs with other functions. Despite its higher sequence similarity to CHSs, DluHKS appears in the non CHS cluster and seems to be most closely related to PinHKS and the heptaketide forming aloesone synthase (ALS) of *Rheum palmatum* (Abe et al., 2004b). This suggests that DluHKS is functionally similar to the two other PKSs and may therefore be able to perform five or six condensation steps with a short starter. However, conclusions drawn from alignments or cladistic analyses can be misleading and need to be confirmed by functional characterization.

Consequently, *DluHKS* was expressed in *E. coli*. The ORF was cloned into the pET-100/D-TOPO vector containing an N-terminal hexahistidine fusion tag. The expression vector was transformed in the host *E. coli* BL21 (DE3). After induction of expression with IPTG, the recombinant protein was purified by immobilized metal affinity chromatography on cobalt resin. SDS–PAGE results are shown in Fig. 4. The purified enzyme gave a band with a molecular mass of 46 kDa which includes the hexahistidine tag and a few amino acids from the vector.

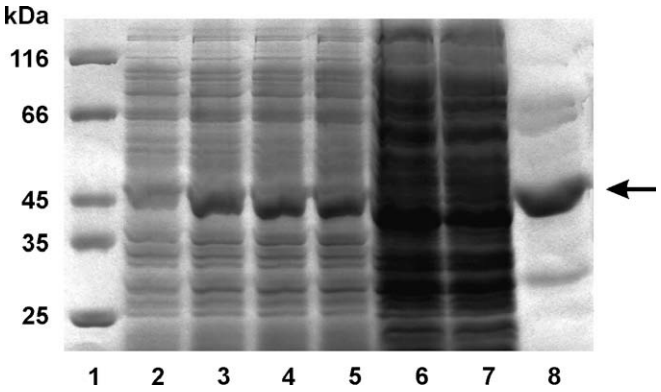

Fig. 4. SDS–PAGE analysis of the purification of recombinant DluHKS. The protein from each individual purification step was applied to a 10% SDS gel and visualized with Coomassie Brilliant Blue R250. Lanes: 1 molecular mass markers (kDa), 2 non-induced *E. coli* cells, 3, 4 and 5 IPTG-induced cells after 2, 4 and 6 h at 24 °C, 6 total cellular lysate, 7 flow-through of affinity column, 8 DluHKS purified by affinity chromatography on cobalt resin. The position of recombinant DluHKS is indicated by an arrow.

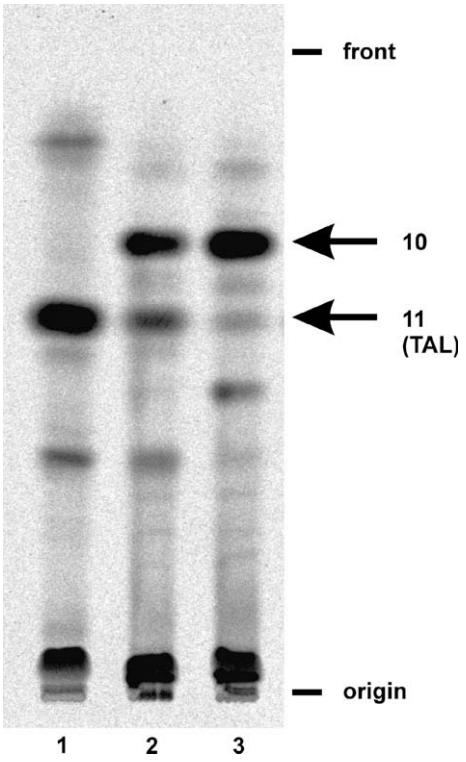

Fig. 5. Radio-TLC analysis of products extracted from PKS assays. Comparison of products obtained with recombinant CalCHS1 (1), PinHKS (2) and DluHKS (3) in incubations with acetyl-CoA **(5)** and [2-^{14}C]malonyl-CoA **(1)**. The compounds identified as triacetate lactone (TAL, **11**) and 6-(2', 4'-dihydroxy-6'-methylphenyl)-4-hydroxy-2-pyrone (**10**) are marked by arrows.

Purified recombinant DluHKS was incubated with acetyl-CoA **(5)** as starter and [2-^{14}C]malonyl-CoA **(1)** as extender unit, and the products extracted from the incubation were analyzed by radio-TLC. For comparison, recombinant PinHKS and CHS1 from *Cassia alata* (CalCHS1) were analyzed under the same conditions. Radio-TLC analysis revealed that PinHKS and DluHKS are functionally similar and synthesized several compounds that comigrated

Table 1
Enzymatic products of DluHKS with different starter CoA esters

Starter CoA ester	Products		
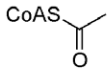 Acetyl-CoA **(5)**	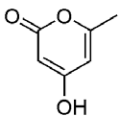 *m/z* 125 $[M-H]^-$ **(11)**	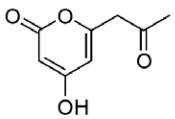 *m/z* 167 $[M-H]^-$ **(12)**	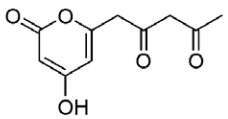 *m/z* 209 $[M-H]^-$ **(13)**
			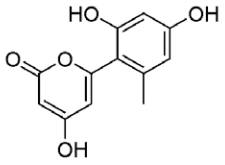 *m/z* 233 $[M-H]^-$ **(10)**
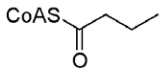 *n*-Butyryl-CoA **(14)**	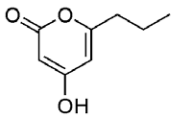 *m/z* 153 $[M-H]^-$ **(15)**	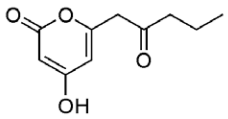 *m/z* 195 $[M-H]^-$ **(16)**	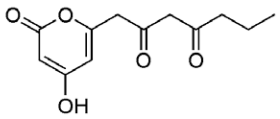 *m/z* 237 $[M-H]^-$ **(17)**
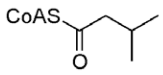 Isovaleryl-CoA **(18)**	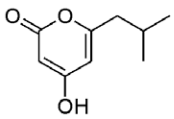 *m/z* 167 $[M-H]^-$ **(19)**	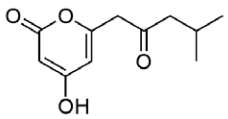 *m/z* 209 $[M-H]^-$ **(20)**	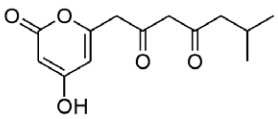 *m/z* 251 $[M-H]^-$ **(21)**
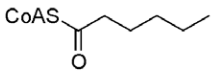 *n*-Hexanoyl-CoA **(22)**	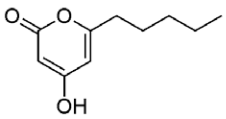 *m/z* 181 $[M-H]^-$ **(23)**	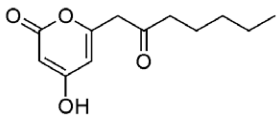 *m/z* 223 $[M-H]^-$ **(24)**	
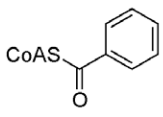 Benzoyl-CoA **(25)**	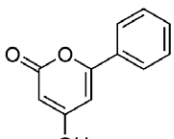 *m/z* 187 $[M-H]^-$ **(26)**	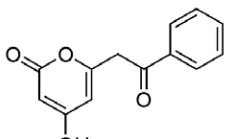 *m/z* 229 $[M-H]^-$ **(27)**	
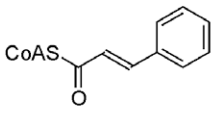 Cinnamoyl-CoA **(28)**	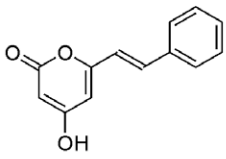 *m/z* 213 $[M-H]^-$ **(29)**	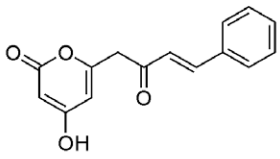 *m/z* 255 $[M-H]^-$ **(30)**	
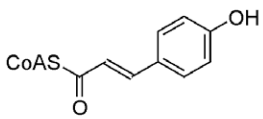 *p*-Coumaroyl-CoA **(2)**	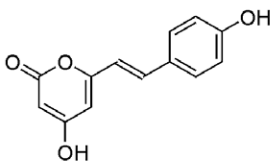 *m/z* 229 $[M-H]^-$ **(31)**	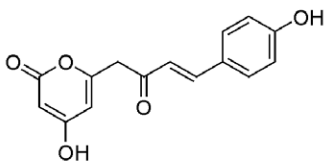 *m/z* 271 $[M-H]^-$ **(32)**	

Table 2
Collision-induced dissociation (CID) mass spectra of enzymatically formed products obtained from the $[M-H]^-$ ions by LC/ESI-MS (RT_{LC} = LC retention time) and elemental composition determined by HR/ESI-MS

Starter CoA ester	Product	Collision energy	Rt_{LC} (min)	$[M-H]^-$ (m/z)	Ions in the negative ion CID mass spectra [*m/z* (rel. int.)]	HR-negative ion ESI-MS (elemental composition)
Acetyl-CoA (**5**)	11		4.74	125		not determined
	12	+15	4.23	167	167 (16), 125 (100), 123 (10), 83 (8), 81 (13), 75 (3), 65 (7)	not determined
	13	+15	6.66	209	209 (1), 125 (100), 123 (4), 81(2)	not determined
	10	+15	12.16	233	233 (24), 191 (14), 189 (100), 165 (41), 147 (54), 145 (3)	*m/z* 233.04516 $[M-H]^-$ (calcd. for $C_{12}H_9O_5^-$ 233.04555)
n-Butyryl-CoA (**14**)	16	+15	8.52	195	195 (13), 151 (14), 125 (100), 123 (7), 109 (11) 83 (4), 65 (4)	*m/z* 195.06584 $[M-H]^-$ (calcd. for $C_{10}H_{11}O_4^-$ 195.06628)
	15	+15	11.33	153	153 (13), 111 (4), 110 (100)	
	17	+15	16.92	237	237 (1), 151 (5), 125 (100), 123 (2), 81 (4)	*m/z* 237.07652 $[M-H]^-$ (calcd. for $C_{12}H_{13}O_5^-$ 237.07685)
Isovaleryl-CoA (**18**)	20	+15	16.59	209	209 (19), 165 (13), 125 (100), 123 (14), 83 (3)	*m/z* 209.08142 $[M-H]^-$ (calcd. for $C_{11}H_{13}O_4^-$ 209.08194)
	19	+20	17.55	167	167 (1), 125 (11), 123 (100), 83 (5)	*m/z* 167.07108 $[M-H]^-$ (calcd. for $C_9H_{11}O_3^-$ 167.07137)
	21	+20	19.34	251	251 (3), 165 (2), 125 (100), 81 (2)	*m/z* 251.09215 $[M-H]^-$ (calcd. for $C_{13}H_{15}O_5^-$ 251.09250)
n-Hexanoyl-CoA (**22**)	24	+15	19.32	223	223 (22), 181 (1), 179 (22), 137 (8), 125 (100), 83 (3)	*m/z* 233.09714 $[M-H]^-$ (calcd. for $C_{12}H_{15}O_4^-$ 233.09758)
	23	+15	19.92	181	181 (14), 139 (5), 137 (100)	*m/z* 181.08657 $[M-H]^-$ (calcd. for $C_{10}H_{13}O_3^-$ 181.08718)
Benzoyl-CoA (**25**)	27	+15	16.53	229	229 (38), 187 (16), 185 (65), 161 (100), 145 (5), 143 (68), 119 (16), 83 (27), 65 (7)	*m/z* 229.05038 $[M-H]^-$ (calcd. for $C_{13}H_9O_4^-$ 229.05063)
	26	+15	17.75	187	187 (24), 145 (5), 143 (100)	*m/z* 187.03965 $[M-H]^-$ (calcd. for $C_{11}H_7O_3^-$ 187.04007)
Cinnamoyl-CoA (**28**)	30	+15	18.90	255	255 (73), 213 (6), 211 (38), 195 (7), 187 (100), 183 (4), 172 (18), 145 (36), 125 (6), 83 (3)	*m/z* 255.06693 $[M-H]^-$ (calcd. For $C_{15}H_{11}O_4^-$ 255.06628)
	29	+15	20.01	213	213 (30), 171 (4), 169 (100), 141 (8), 139 (2)	*m/z* 213.05525 $[M-H]^-$ (calcd. for $C_{13}H_9O_3^-$ 213.05572)
p-Coumaroyl-CoA (**2**)	32	+15	14.74	271	271 (64), 253 (7), 229 (37), 227 (42), 211 (56), 203 (75), 185 (13), 179 (8), 161 (19), 145 (100), 125 (40)	*m/z* 271.06114 $[M-H]^-$ (calcd. for $C_{15}H_{11}O_5^-$ 271.06120)
	31	+15	16.35	229	229 (37), 187 (5), 185 (100), 157 (3), 143 (26)	*m/z* 229.05031 $[M-H]^-$ (calcd. for $C_{13}H_9O_4^-$ 229.05063)
	31	−20		231[a]	231 (25), 213 (12), 203 (23), 185 (27), 171 (19), 157 (38), 147 (100), 145 (6), 129 (5), 121 (11), 107 (4), 69 (9)[b]	

[a] $[M+H]^+$.
[b] Positive ion CIDMS.

(Fig. 5). In contrast, CalCHS1 produced mainly triacetate lactone (TAL, compound **11**, Table 1) from acetyl-CoA **(5)** and malonyl-CoA **(1)**.

The major product of DluHKS is the hexaketide 6-(2',4'-dihydroxy-6'-methylphenyl)-4-hydroxy-2-pyrone (compound **10**, Table 1). This compound was identified on the radio-TLC plate by co-chromatography with an authentic standard prepared by hydrolysis of aloenin A. With the exception of TAL (**11**), which could be tentatively identified by co-migration with the main product of CalCHS1, and the hexaketide **10**, the identity of all other radiolabeled products of DluHKS in the TLC analysis could not be determined because authentic standards were not available.

If the assay mixture was not stopped by acidification and directly spotted onto the TLC plate, most of the radioactive products remained at the origin or close to it (data not shown). This suggests that several products are only formed after acidification. Most likely, the recombinant PinHKS and DluHKS produce linear polyketides that undergo cyclization at low pH.

To further identify the products formed, DluHKS was incubated with unlabeled acetyl-CoA **(5)** and malonyl-CoA **(1)** in scaled up assays. The products were analyzed by HPLC, LC/ESI-MS and GC/MS (HPLC and GC/MS data not shown). By comparison with the CID (collision induced dissociation) mass spectra of the products of PinHKS (Springob et al., 2007), the polyketides synthesized by DluHKS were identified as 4-hydroxy-6-methyl-2-pyrone (TAL, **11**) and 6-acetonyl-4-hydroxy-2-pyrone (**12**), 4-hydroxy-6-(2',4'-dioxo-pentyl)-pyrone (**13**) and 6-(2',4'-dihydroxy-6'-methylphenyl)-4-hydroxy-2-pyrone (**10**) (Tables 1 and 2). However, one product of PinHKS, 4-hydroxy-6-(2',4'-trioxo-heptyl)-pyrone, was not found to be synthesized by DluHKS.

Recombinant DluHKS does not depend on acetyl-CoA **(5)** as start substrate, because it can also use malonyl-CoA **(1)** efficiently. However, in comparison to assays without acetyl-CoA **(5)**, 22% higher yields ($p = 0.057$) of the hexaketide phenylpyrone (compound **10**) were obtained when acetyl-CoA **(5)** was added to the assay mixture. Even in the presence of 100-fold higher concentrations of unlabeled malonyl-CoA **(1)**, [1-^{14}C]acetyl-CoA **(5)** was utilized as starter substrate.

Since the hexaketide (compound **10**) is the main product of recombinant DluHKS with acetyl-CoA **(5)** as starter substrate, the kinetic parameters of its formation were investigated. Formation of **10** is linear during a period of 20 min using protein concentrations up to 2 μg/100 μl. DluHKS showed a pH optimum for the formation of **10** at pH 6.0 and 6.5 and a temperature optimum at 45 °C. K_M values of 31 μM for acetyl-CoA **(5)** and 83 μM for malonyl-CoA **(1)** were found. These values are about 10–20-fold higher than the K_M values determined for the starter and extender substrates (*p*-coumaroyl-CoA, **2**, and malonyl-CoA, **1**) of CHSs and STSs (Schüz et al., 1983; Schöppner and Kindl, 1984; Jez et al., 2000b). However, comparatively high K_M values for malonyl-CoA **(1)** were also reported for *Aloe arborescens* pentaketide chromone synthase (PCS) and octaketide synthase, two PKSs that catalyze more condensation steps than most other type III PKSs (Abe et al., 2005a,b).

To determine the activity of DluHKS with other starter molecules, the recombinant enzyme was incubated with [2-^{14}C]malonyl-CoA **(1)** and the CoA esters acetyl-CoA **(5)**, *n*-butyryl-CoA **(14)**, isovaleryl-CoA **(18)**, *n*-hexanoyl-CoA **(22)**, benzoyl-CoA **(25)**, cinnamoyl-CoA **(28)** and *p*-coumaroyl-CoA **(2)**. The resulting radioactive products were resolved by reversed-phase TLC (data not shown). DluHKS showed relaxed starter unit specificity, accepted both aliphatic and aromatic CoA esters as primers for polyketide synthesis and produced multiple products from each. To compare the amount of products formed from acetyl-CoA with the other starter CoA esters, the total incorporation of radioactivity from labeled malonyl-CoA **(1)** was used for quantification. Under the experimental conditions used, highest incorporation of [2-^{14}C]malonyl-CoA **(1)** into products was found with *n*-butyryl-CoA **(14)**, isovaleryl-CoA **(18)** and *n*-hexanoyl-CoA **(22)**. For comparison, a three times lower incorporation of [2-^{14}C]malonyl-CoA **(1)** was determined with acetyl-CoA **(5)** as primer unit. This result suggests that acetyl-CoA **(5)** might not be the physiological substrate. However, these assays with different start substrates were carried out under conditions used by Samappito et al. (2002), which are not optimized for the formation of the hexaketide (**10**). In addition, there are reports on type III PKSs that show higher affinity to unnatural substrates than to their physiological primer unit (Abe et al., 2004a). Given the substrate promiscuity of type III PKSs, not only the affinity for a certain substrate, but also its availability will determine the physiological function of the enzyme.

The products synthesized from alternative starter CoA esters could not be identified by radio-TLC analysis due to the lack of authentic standards. Consequently, scaled up assays with unlabeled substrates were performed, and the reaction products were analyzed by LC/ESI-MS/MS. High resolution (HR)/ESI-MS analysis was carried out to determine the elemental composition of the products. The chemical structures of the products are summarized in Table 1 and the corresponding mass-spectral data are shown in Table 2. Recombinant DluHKS produced tri-, tetra- and pentaketide pyrones with the small primer units *n*-butyryl-CoA **(14)** and isovaleryl-CoA **(18)**. With the larger starter CoA esters hexanoyl-CoA **(22)**, benzoyl-CoA **(25)**, cinnamoyl-CoA **(28)** and *p*-coumaroyl-CoA **(2)** only di- and triketide pyrones were formed. *Bis*-noryangonin (**31**), the triketide pyrone from the starter *p*-coumaroyl-CoA **(2)**, was identified by its parent ions $[M+H]^+$ (*m/z* 231) and $[M-H]^-$ (*m/z* 229), respectively (Table 2). The electrospray CID spectrum of the $[M-H]^-$ ion (*m/z* 229) displayed key ions at *m/z* 187 $[M-H-CH_2CO]$ and *m/z* 185 $[M-H-CO_2]$, and the CID spectrum of the $[M+H]^+$ ion (*m/z* 231) yielded a characteristic fragment at *m/z* 147 (Samappito et al., 2002).

Acylphloroglucinol derivatives or stilbenes, the typical products of CHSs and STSs, could not be detected with any of the starters. Hence, the product spectrum of DluHKS is similar to that obtained with PinHKS (Springob et al., 2007).

It is known from previous investigations that the active site cavity of type III PKSs acts as size-based filter and determines starter substrate specificity, number of possible extensions and type of cyclization. Therefore, changes in amino acid residues lining the active site can lead to enzymes with altered product profiles (Jez et al., 2000a; Abe et al., 2006a,b). In order to find out whether modifications in the active site can explain the unusual properties of DluHKS and PinHKS, the enzymes were modeled based on the structure of *M. sativa* CHS2 complexed with resveratrol (PDB code 1CGZ) using the SWISS-MODEL protein modeling server.

Although the overall three-dimensional fold of DluHKS and PinHKS is very similar to that of CHS, several amino acids lining the active site cavity of the HKSs are changed relative to *M. sativa* CHS2 (Fig. 6). For example, Ser133, Gly256 and Ser338 (numbering according to *M. sativa* CHS2), which are highly conserved in CHSs, are substituted with Ala, Leu and Thr, respectively, in the two HKSs. In addition, Thr194, Val196 and Thr197, three amino acids at the bottom of the active site of CHS, are replaced by Phe202, Phe204 and Ala205 in PinHKS. DluHKS, instead, contains Thr192, Ile194 and Phe195 at the respective positions. Although the two HKSs show a different amino acid substitution pattern in this case, most substitutions introduce bulkier residues suggesting that the available space may be reduced in comparison with CHS. Several type III PKSs functionally divergent from CHS contain similar amino acid exchanges. In particular, mutations of T197, G256, and S338 were shown to modulate PKS activity. Analysis of the three-dimensional structures of *Gerbera hybrida* 2-pyrone synthase (2-PS) and *A. arborescens* PCS demonstrated that the small to large exchange of amino acids corresponding to T197, G256 and S338 in

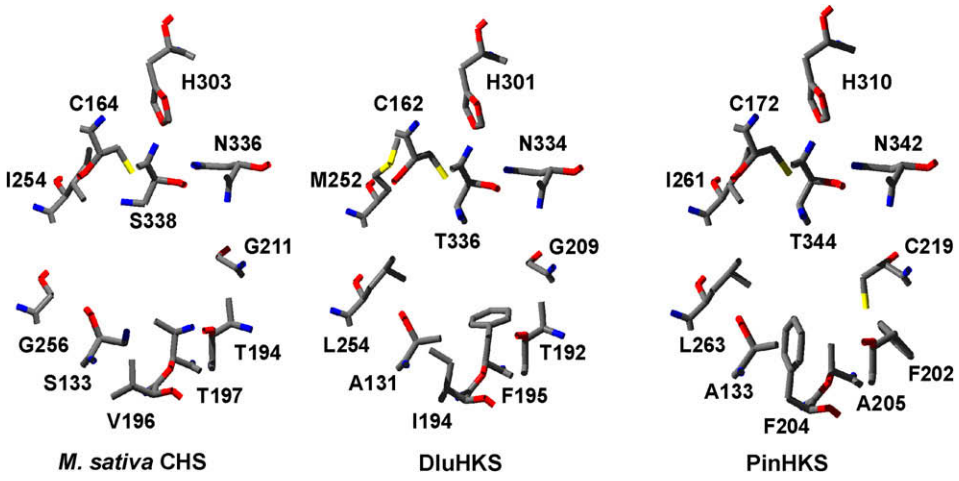

Fig. 6. Models of the active sites of *M. sativa* CHS2, DluHKS and PinHKS. The structures of DluHKS and PinHKS were modeled based on the structure of *M. sativa* CHS2 complexed with resveratrol (PDB code 1CGZ, resveratrol not shown).

CHS reduces the volume of the active site cavity (Jez et al., 2000a; Morita et al., 2007). Similarly, *Streptomyces coelicolor* 1,3,6,8-tetrahydroxynaphthalene synthase (THNS) contains Tyr instead of G256, which leads to a horizontal restriction of the cavity and a preference of small starter molecules. T197 and S338, however, are replaced by smaller amino acids in THNS. This causes a downward expansion that allows four extensions with malonyl-CoA **(1)** (Austin et al., 2004).

The reduced space available in the active site can explain the preference of DluHKS for smaller CoA esters. However, it is still unclear why the HKSs can catalyze more condensations with malonyl-CoA **(1)** than CHS. Most likely, other amino acid exchanges, for example the S133A substitution, which occurs in DluHKS and PinHKS, might increase the space available for the growing polyketide chain in the active site of DluHKS. The importance of the amino acid residue in position 133 and its neighbors was shown with *Ruta graveolens* acridone synthase 2 (ACS2). Site-directed mutagenesis of S132, A133 and V265 into Thr, Ser and Phe, the corresponding residues of *M. sativa* CHS2, converted ACS2 into a functional CHS (Lukačin et al., 2001).

Two other interesting amino acid exchanges relative to CHS occur only in PinHKS, but not in DluHKS. Gly211 and Phe265 are replaced with Cys and Ile, respectively. These variations do not influence the ability to synthesize hexaketides from six acetate units, however, they might be responsible for the slightly different product pattern of the two enzymes.

This study had the aim to isolate a PKS from *D. lusitanicum* that catalyzes the formation of naphthalenes or naphthoquinones. However, in analogy to the previously described PinHKS, the recombinant DluHKS could not catalyze the formation of naphthalenes, but produced α-pyrones from an acetyl-CoA **(5)** starter and two to five malonyl-CoA **(1)** extender units. To the best of our knowledge, *D. lusitanicum* does not produce any of the pyrone-type compounds detected (Table 1). On the other hand, we could not observe naphthalene formation in *in vitro* PKS assays with crude protein extracts from *D. lusitanicum* callus cultures (data not shown). Nevertheless, DluHKS performs five condensations as required for the synthesis of the naphthoquinone skeleton. Therefore, it appears possible that DluHKS provides the backbone of these metabolites, and further downstream processing steps convert the intermediate into naphthoquinones.

Most likely, a reductase is required that removes the oxygen at the third acetate unit. The only polyketide reductase characterized from plants so far is chalcone reductase. For other pathways, e.g. the biosynthesis of stilbenecarboxylates and anthrones, the presence of such an enzyme has been hypothesized (Eckermann et al., 2003; Abe et al., 2005b). In the case of naphthoquinone biosynthesis, additional evidence for the presence of a reductase can be derived from biomimetic syntheses of acetate-derived naphthalenes and isoquinolines (Bringmann, 1985). A chemically prepared 2,4,6,8,10-pentaketone spontaneously undergoes aldol cyclization between C-2 and C-7, yielding a methylresorcinol ring identical to that of the hexaketide **10**. In contrast, if the oxygen at C-6 of the pentaketone is protected, e.g., as acetal, the condensation occurs between C-4 and C-9, a cyclization identical to the postulated first ring closure in naphthoquinone biosynthesis (Fig. 1, numbering of carbon atoms according to polyketide literature). Interestingly, the oxygen at C-7 of the hexaketide intermediate (Fig. 1), corresponding to C-6 of the pentaketone, is removed by reduction in all naphthoquinones of polyketide origin. Although the cited cyclization experiments were performed with a pentaketone and not with the herein postulated hexaketide intermediate, the chemistry of the cyclization reaction is valid for both molecules. For the biosynthesis of naphthoquinones this suggests that the cyclization of the first ring between C-4 and C-9 occurs after the oxygen at C-7 has been reduced.

The postulation of enzymes acting downstream of DluHKS *in vivo* also implies shuttling of a hexaketide intermediate and possibly interactions with the other proteins. The active site of type III PKSs is buried in the enzyme, but it is only separated from the outside solution by a β-strand finger. Interactions with other proteins may displace this thin wall and thus reshape the active site cavity (Austin and Noel, 2003). The suggestion of accessory proteins for naphthoquinone biosynthesis remains highly speculative, but the EST library of *D. lusitanicum* callus cultures may provide a good base to identify and study such additional co-factors.

It is still possible that DluHKS is involved in a different biosynthetic pathway. Moreover, the recombinant enzyme may produce naphthalenes under different conditions than applied in the *in vitro* assays. Since the enzyme described is the second HKS isolated from a naphthoquinone-producing plant, however, it becomes more likely that this kind of PKS provides the backbone of naphthoquinones.

3. Conclusion

We have isolated a PKS that synthesizes α-pyrones from three to six acetate units. The enzyme shows the promiscuous substrate

acceptance typical of most known type III PKS, although a clear-cut answer about its physiological function could not be provided. However, our results suggest that enzymes like DluHKS and PinHKS that can condense six acetate units catalyze the first step of naphthoquinone biosynthesis.

4. Experimental

4.1. Chemicals

Acetyl-CoA, malonyl-CoA **(1)**, *n*-butyryl-CoA **(14)**, isovaleryl-CoA **(18)**, *n*-hexanoyl-CoA **(22)**, benzoyl-CoA **(25)**, and plumbagin **(8)** were purchased from Sigma (Munich, Germany). [1-^{14}C]acetyl-CoA **(5)** (4 mCi/mmol) and [2-^{14}C]malonyl-CoA **(1)** (55 mCi/mmol) were obtained from Biotrend Chemikalien (Cologne, Germany). *p*-Coumaroyl-CoA **(2)** and cinnamoyl-CoA **(28)** were kindly provided by Dagmar Knöfel at the Leibniz-Institut für Pflanzenbiochemie (IPB), Halle (Saale), Germany. Aloenin A was purchased from Phytoplan GmbH (Heidelberg, Germany).

4.2. Plant material

Callus cultures of *D. lusitanicum* were grown on LS medium supplemented with 0.186 mg/l α-naphtylacetic acid and 0.22 mg/l 2,4-dichlorphenoxy acetic acid. The callus was subcultured every 4 weeks and maintained under a 16 h photoperiod at 24 °C.

4.3. cDNA library construction

Total RNA was isolated from callus cultures of *D. lusitanicum* as described by Salzman et al. (1999). Poly (A)$^+$ RNA was obtained from total RNA using the Oligotex™ mRNA Kit (Qiagen, Hilden, Germany), and synthesis of first- and second-strand cDNA was carried out according to the instructions of the CloneMiner™ cDNA Library Construction Kit (Invitrogen, Karlsruhe, Germany). The double strand cDNA was ligated with the *att*B adapter and size fractionated to remove excess primer, adapters, and small cDNAs by CC (Sephacryl® S-500 HR resin). The *att*B-flanked cDNA was ligated into pDONR™222 (*att*P containing vector, Invitrogen) with BP Clonase™ enzyme mix through the Gateway® BP recombination reaction and transformed into competent *Escherichia coli* ElectroMax™ DH10B™ T1 Phage Resistant Cells (Invitrogen). The non-amplified *D. lusitanicum* cDNA library contained 5×10^6 colony forming units in a total volume of 12 ml.

4.4. Expressed sequence tag (EST) analysis of cDNA library

Hundred microlitre of a 1:100 dilution of the *D. lusitanicum* cDNA library was plated onto prewarmed LB plates containing 50 μg/ml kamamycin and incubated overnight at 37 °C. Single colonies were picked and grown in 50 μl Luria–Bertani (LB) containing kamamycin at 37 °C overnight. cDNA inserts were amplified from the bacterial cultures by PCR using an M13 uni primer: 5'-ACG ACG TTG TAA AAC GAC GGC CAG-3' and an M13 reverse primer: 5'-TTC ACA CAG GAA ACA GCT ATG ACC-3'. The PCR reaction was performed in 50 μl total volume containing 1–2 μl of the bacterial culture, 5 μl of 10× PCR buffer with 15 mM $MgCl_2$, 1 μl dNTPmix, 1 μl of 10 μM M13 uni primer and 1 μl of 10 μM M13 reverse primer under the following PCR conditions: 5 min at 94 °C for 1 cycle, then 30 cycles of 94 °C for 30 s, 50 °C for 30 s, 72 °C for 30 s. This was followed by an additional elongation step at 72 °C for 5 min. The PCR products were sequenced using the M13 uni primer and the BigDye® Terminator v3.1 Cycle sequencing Kit (Applied Biosystems, Darmstadt, Germany). After removal of excess dye by size exclusion chromatography, sequencing reactions were run on the ABI PRISM 3100-Avant Genetic Analyzer (Applied Biosystems).

The EST sequences were trimmed for vector contamination and assembled with the SeqManII™ module of the Lasergene software package (DNASTAR Inc., Madison, WI, USA) to obtain individual contigs. The assembling parameters included a minimum match size of 20 and a minimum match percentage of 80. Each contig was subjected to an automated BlastX search using DNASIS™ (Hitachi Software Engineering, Berlin Germany).

4.5. 5' RACE PCR for full-length cDNA synthesis

The missing 5' end of the *DluHKS* cDNA was isolated by 5'-rapid amplification of cDNA ends (5' RACE) using the BD SMART™ RACE cDNA Amplification Kit (Clontech, Heidelberg, Germany). Total RNA of *D. lusitanicum* callus cultures was used as template for first-strand cDNA synthesis. 5' RACE PCR was performed using the gene-specific primer 5'-GTA CTC GCT GAG CAC GTA TCG ACT CTCC-3' and the universal primer mix (UPM) supplied by the manufacturer to amplify an approximately 1.2 kb DNA fragment. Cycling conditions consisted of 5 cycles of 94 °C, 30 s; 68 °C; 30 s and 72 °C, 3 min, followed by 5 cycles of 94 °C, 30 s; 66 °C, 30 s and 72 °C, 3 min, followed by 5 cycles of 94 °C, 30 s; 64 °C, 30 s and 72 °C, 3 min, followed by 25 cycles of 94 °C, 30 s; 62 °C, 30 s and 72 °C, 3 min and followed by 5 min at 72 °C. The 5' RACE PCR product was purified by gel electrophoresis and extracted using the Mini Elute Gel Extraction Kit (Qiagen), ligated into pGEM® T-Easy (Promega, Madison, WI, USA) and sequenced.

4.6. Functional expression in E. coli

To express the *DluHKS* full-length cDNA in *E. coli*, the open reading frame was cloned into pET-100D/TOPO (Invitrogen), which contains a hexahistidine N-terminal fusion tag. Amplification was performed using the forward primer: 5'-CAC CAT GGC ATT TGT GGA GGG AAT GGG GAAG-3' (the 4 underlined nucleotides anneal to the GTGG overhang of the pET100/D-TOPO vector) and the reverse primer: 5'-TTA GTT GTT TAT AGG GAA GCT TCG CAA TAC-3' with *D. lusitanicum* first-strand cDNA as template and *Pfu* DNA polymerase (Fermentas, St.Leon-Rot, Germany). The 1.2 kb PCR product was gel-purified and ligated into pET-100D/TOPO. The sequence of the resulting construct DluHKS:pET-100D/TOPO was confirmed, and the expression plasmid was transformed into *E. coli* BL21 Star™ (DE3) One Shot® cells (Invitrogen).

E. coli harboring DluHKS:pET-100D/TOPO were grown at 37 °C in LB medium containing 50 μg/ml ampicillin until $A_{600} \sim 0.6$. Protein expression was induced with 1.0 mM isopropyl-1-thio-β-D-galactopyranoside, and the culture was grown at 24 °C for 6 h. *E. coli* cells were harvested, and recombinant DluHKS was purified by following procedures described previously (Samappito et al., 2002, 2003).

4.7. Polyketide synthase assay

The standard reaction mixture contained 100 mM K-Pi buffer (pH 6.5), 50 μM acetyl-CoA **(5)**, 100 μM [2-^{14}C]malonyl-CoA **(1)** (70,000 dpm) and 0.5–5.0 μg recombinant enzyme in a 100 μl reaction. The assays were incubated for 15 min at 45 °C, stopped by addition of 10 μl of 1 M HCl, incubated for an additional 15 min at 45 °C to convert all uncyclized products into lactones, and extracted with EtOAc (3 × 500 μl). The organic phases were dried, and products were separated by TLC on silica gel with EtOAc–MeOH–H_2O (100:16.5:13.5; v/v). The ^{14}C-labeled products were visualized by phosphorimagery (Typhoon 9410, Amersham Biosciences). TAL (**11**) was identified by comparison with the products of chalcone synthase from *Cassia alata* (CalCHS1) (Samappito et al.,

2002), incubated under the same conditions as DluHKS, and 6-(2',4'-dihydroxy-6'-methylphenyl)-4-hydroxy-2-pyrone (**10**) was identified as described in Section 4.10.

The kinetic parameters of DluHKS were determined by quantifying the spot of the hexaketide (**10**) on the TLC by phosphorimaging. All assays were carried out in triplicate. The K_M for malonyl-CoA **(1)** was determined using 50 μM acetyl-CoA **(5)** and 5–200 μM [2-^{14}C]malonyl-CoA **(1)**. To determine the K_M of acetyl-CoA **(5)**, the incubations contained 3–81 μM [1-^{14}C]acetyl-CoA **(5)** and 500 μM unlabeled malonyl-CoA **(1)**. As standard for quantification, 1 μl of 1 mM [2-^{14}C]malonyl-CoA **(1)** (7000 dpm/μl) was spotted on each TLC plate. For the K_M of acetyl-CoA **(5)**, 1 μl of 1.6 mM [1-^{14}C]acetyl-CoA **(5)** (14,000 dpm/μl) and 1 μl of 0.17 mM [1-^{14}C]acetyl-CoA **(5)** (1460 dpm/μl) were spotted on the TLC plates as standards.

To compare the activity of DluHKS with acetyl-CoA **(5)** and various larger starter CoA esters, the incubations were performed as described by Samappito et al., 2002. For quantitative evaluation of these assays, the incorporation of [2-^{14}C]malonyl-CoA **(1)** into all reaction products from one starter substrate was quantified by phosphorimaging. The enzyme assay contained 100 mM HEPES buffer (pH 7.0), 20 μM starter CoA, 70 μM [2-^{14}C]malonyl-CoA **(1)** (80,000 dpm), and 5 μg polyketide synthase in a 50 μl reaction volume. The assay mixture was incubated at 30 °C for 30 min. The reaction was stopped by the addition of 5 μl 10% (v/v) HCl and was extracted with EtOAc (2 × 100 μl). The combined organic phases were evaporated to dryness and products separated by RP-18 thin layer chromatography (Merck) and developed in MeOH–H_2O–HOAc (75:25:1; v/v). Each assay was carried out in duplicate.

4.8. LC–MS and high resolution MS analysis of enzymatic products

To identify the enzymatic products in the incubation mixtures containing various starter-CoA esters, 5 scaled-up 200 μl reactions were carried out containing 100 mM HEPES (pH 7.0), 50 μM starter-CoA ester, 100 μM malonyl-CoA **(1)** and 50 μg purified protein. After incubation for 1 h at 30 °C, the mixtures were acidified and extracted with EtOAc (2 × 400 μl). The combined organic phases were evaporated to dryness, and the residue was dissolved in MeOH and subjected to LC–MS analysis. Negative and positive ion electrospray ionization (ESI) mass spectra were obtained with a Finnigan MAT TSQ 7000 instrument coupled with a Surveyor MicroLC system equipped with an RP18-column (5 μm, 1 × 100 mm, SepServ, Berlin) as described previously (Samappito et al., 2002; Springob et al., 2007).

The high resolution negative ion ESI mass spectra were obtained with a Bruker Apex III Fourier transform ion cyclotron resonance (FT-ICR) mass spectrometer (Bruker Daltonics, Billerica, USA) equipped with an Infinity™ cell, a 7.0 T superconducting magnet (Bruker, Karlsruhe, Germany), an RF-only hexapole ion guide and an external electrospray ion source (Agilent, off axis spray, voltages: endplate, 3.700 V; capillary, 4.400 V; capillary exit, −70 V; skimmer 1, −10 V; skimmer 2, −8 V). Nitrogen was used as drying gas at 150 °C. The sample solutions were introduced continuously via a syringe pump with a flow rate of 120 μl/ h. All data were acquired with 256k data points and zero filled to 1024k by averaging 32 scans as described previously (Springob et al., 2007).

4.9. HPLC analysis

For HPLC separations a Merck-Hitachi HPLC system equipped with an AS-4000A Autosampler, an L-6200A Pump, an L-4500A Diode Array Detector and a Lichrospher 60, RP-select B column (250 × 4 mm, 5 μm) was used (Merck KGaA, Darmstadt, Germany). The solvent system consisted of (A) H_2O–CH_3CN (2:98; v/v) and (B) H_2O–CH_3CN (98:2; v/v) each with 0.2% HOAc, with the following gradient: from 0% B to 60% B in 25 min, 25–30 min 60% B, 30–32 min 60–100% B, 32–35 min 100% B at a flow rate of 1 ml min^{-1}. The detection wavelength was set to 300 nm.

4.10. Preparation of 6-(2',4'-dihydroxy-6'-methylphenyl)-4-hydroxy-2-pyrone (10)

Compound **10** was obtained by hydrolysis of aloenin A (6-(2'-*O*-β-D-glucopyranosyl-4'-hydroxy-6'-methylphenyl)-4-methoxy-2-pyrone) in MeOH–H_2O–HCl (80:17:3; v/v) as described previously (Springob et al., 2007). Although this yielded mainly 6-(2',4'-dihydroxy-6'-methylphenyl)-4-methoxy-2-pyrone, **10** was obtained as minor by-product and could be purified by HPLC (R_t = 15.9 min) using the conditions described under Section 4.9. The identity of **10** was confirmed by LC/ESI-MS.

Acknowledgements

We thank Verona Dietl, Christine Kuhnt and Dagmar Knöfel (Leibniz-Institut für Pflanzenbiochemie, Halle, Germany) for technical assistance and Dr. Joseph M. Jez (Donald Danforth Plant Science Center, St. Louis, MO, USA) for his help in preparing the models of DluHKS and PinHKS. A. Jindaprasert was supported by the Royal Golden Jubilee Ph.D. program, Thailand Research Fund (RGJ-TRF), the German Academic Exchange Service (DAAD), and Thailand's National Center for Genetic Engineering and Biotechnology (BIOTEC, Grant No. 2/2545). Financial support by the DFG priority program SPP1152: "Evolution of metabolic diversity" (KU990/5-2) is gratefully acknowledged.

References

Abe, I., Morita, H., Nomura, A., Noguchi, H., 2000. Substrate specificity of chalcone synthase: enzymatic formation of unnatural polyketides from synthetic cinnamoyl-CoA analogues. J. Am. Chem. Soc. 122, 11242–11243.

Abe, I., Watanabe, T., Noguchi, H., 2004a. Enzymatic formation of long-chain polyketide pyrones by plant type III polyketide synthases. Phytochemistry 65, 2447–2453.

Abe, I., Utsumi, Y., Oguro, S., Noguchi, H., 2004b. The first plant type III polyketide synthase that catalyzes formation of aromatic heptaketide. FEBS Lett. 562, 171–176.

Abe, I., Utsumi, Y., Oguro, S., Morita, H., Sano, Y., Noguchi, H., 2005a. A plant type III polyketide synthase that produces pentaketide chromone. J. Am. Chem. Soc. 127, 1362–1363.

Abe, I., Oguro, S., Utsumi, Y., Sano, Y., Noguchi, H., 2005b. Engineered biosynthesis of plant polyketides: chain length control in an octaketide-producing plant type III polyketide synthase. J. Am. Chem. Soc. 127, 12709–12716.

Abe, I., Watanabe, T., Morita, H., Kohno, T., Noguchi, H., 2006a. Engineered biosynthesis of plant polyketides: manipulation of chalcone synthase. Org. Lett. 8, 499–502.

Abe, I., Watanabe, T., Lou, W., Noguchi, H., 2006b. Active site residues governing substrate selectivity and polyketide chain length in aloesone synthase. FEBS J. 273, 208–218.

Austin, M.B., Noel, J.P., 2003. The chalcone synthase superfamily of type III polyketide synthases. Nat. Prod. Rep. 20, 79–110.

Austin, M.B., Izumikawa, M., Bowman, M.E., Udwary, D.W., Ferrer, J.L., Moore, B., Noel, J.P., 2004. Crystal structure of a bacterial type III polyketide synthase and enzymatic control of reactive polyketide intermediates. J. Biol. Chem. 279, 45162–45174.

Bringmann, G., 1985. Acetogenine Isochinolin-Alkaloide, 6. Aufbau und Cyclisierung zentral modifizierter β-Pentaketone: Synthese monocyclischer Isochinolinalkaloid-Vorstufen. Liebigs Ann. Chem. 1985, 2105–2115.

Bringmann, G., Schlauer, J., Rückert, M., Wiesen, B., Ehrenfeld, K., Proksch, P., 1999. Host-derived acetogenins involved in the incompatible parasitic relationship between *Cuscuta reflexa* and *Ancistrocladus heyneanus*. Plant Biol. 1, 581–584.

Bringmann, G., Rischer, H., Wohlfahrt, M., Schlauer, J., Aké Assi, L., 2000. Droserone from cell cultures of *Triphyophyllum peltatum* (Dioncophyllaceae) and its biosynthetic origin. Phytochemistry 53, 339–343.

Bringmann, G., Feineis, D., 2001. Stress-related polyketide metabolism of Dioncophyllaceae and Ancistrocladaceae. J. Exp. Bot. 52, 2015–2022.

Didry, N., Dubreuil, L., Pinkas, M., 1994. Activity of anthraquinonic and naphthoquinonic compounds on oral bacteria. Pharmazie 49, 681–683.

Dornbos Jr., D.L., Spencer, G.F., 1990. Natural products phytotoxicity. A bioassay for small quantities of slightly water-soluble compounds. J. Chem. Ecol. 16, 339–352.

Durand, R., Zenk, M.H., 1971. Biosynthesis of plumbagin (5-hydroxy-2-methyl-1,4-naphthoquinone) via the acetate pathway in higher plants. Tetrahedron Lett. 12, 3009–3012.

Durand, R., Zenk, M.H., 1974. Enzymes of the homogentisate ring-cleavage pathway in cell suspension cultures of higher plants. Phytochemistry 13, 1483–1492.

Durga, R., Sridhar, P., Polasa, H., 1990. Effects of plumbagin on antibiotic resistance in bacteria. Indian J. Med. Res. 91, 18–20.

Eckermann, C., Schröder, G., Eckermann, S., Strack, D., Schmidt, J., Schneider, B., Schröder, J., 2003. Stilbenecarboxylate biosynthesis: a new function in the family of chalcone synthase-related proteins. Phytochemistry 62, 271–286.

Ferrer, J.L., Jez, J.M., Bowman, M.E., Dixon, R.A., Noel, J.P., 1999. Structure of chalcone synthase and the molecular basis of plant polyketide biosynthesis. Nat. Struct. Biol. 6, 775–784.

Heubl, G., Bringmann, G., Meimberg, H., 2006. Molecular phylogeny and character evolution of carnivorous plant families in Caryophyllales – revisited. Plant Biol. 8, 821–830.

Higa, M., Ogihara, K., Yogi, S., 1998. Bioactive naphthoquinone derivatives from *Diospyros maritima* Blume. Chem. Pharm. Bull. 46, 1189–1193.

Inouye, H., Ueda, S., Inoue, K., Matsumura, K., 1979. Biosynthesis of shikonin in callus cultures of *Lithospermum erythrorhizon*. Phytochemistry 18, 1301–1308.

Jez, J.M., Austin, M.B., Ferrer, J.L., Bowman, M.E., Schröder, J., Noel, J.P., 2000a. Structural control of polyketide formation in plant-specific polyketide synthases. Chem. Biol. 7, 919–930.

Jez, J.M., Ferrer, J.L., Bowman, M.E., Dixon, R.A., Noel, J.P., 2000b. Dissection of malonyl-coenzyme A decarboxylation from polyketide formation in the reaction mechanism of a plant polyketide synthase. Biochemistry 39, 890–902.

Leistner, E., 1999. In: Barton, D.H.R., Nakanishi, K., Meth-Cohn, O. (Eds.), Comprehensive Natural Products Chemistry, vol. 1. Pergamon, Oxford, pp. 609–622.

Likhitwitayawuid, K., Kaewamatawong, R., Ruangrungsi, N., Krungkrai, J., 1998. Antimalarial naphthoquinones from *Nepenthes thorelii*. Planta Med. 64, 237–241.

Lukačin, R., Schreiner, S., Matern, U., 2001. Transformation of acridone synthase to chalcone synthase. FEBS Lett. 508, 413–417.

Meimberg, H., Dittrich, P., Bringmann, G., Schlauer, J., Heubl, G., 2000. Molecular phylogeny of Caryophyllidae s. l. based on *matK* sequences with special emphasis on carnivorous taxa. Plant Biol. 2, 218–228.

Morita, H., Takahashi, Y., Noguchi, H., Abe, I., 2000. Enzymatic formation of unnatural aromatic polyketides by chalcone synthase. Biochem. Biophys. Res. Commun. 279, 190–195.

Morita, H., Kondo, S., Oguro, S., Noguchi, H., Sugio, S., Abe, I., Kohno, T., 2007. Structural insight into chain-length control and product specificity of pentaketide chromone synthase from *Aloe arborescens*. Chem. Biol. 14, 359–369.

Peters, K., Peters, E.M., von Schnering, H.G., Bringmann, G., Kehr, C., Haller, R.D., Bär, S., Isahakia, M.A., Robertson, S.A., 1995. Crystal structure of droserone in 'biogenic crystals' found under the stem bark of *Ancistrocladus robertsoniorum*. Z. Kristallogr. 210, 290–291.

Salzman, R.A., Fujita, T., Zhu-Salzman, K., Hasegawa, P.M., Bressan, R.A., 1999. An improved RNA isolation method for plant tissues containing high levels of phenolic compounds or carbohydrates. Plant Mol. Biol. Reporter 17, 11–17.

Samappito, S., Page, J.E., Schmidt, J., De-Eknamkul, W., Kutchan, T.M., 2002. Molecular characterization of root-specific chalcone synthases from *Cassia alata*. Planta 216, 64–71.

Samappito, S., Page, J.E., Schmidt, J., De-Eknamkul, W., Kutchan, T.M., 2003. Aromatic and pyrone polyketides synthesized by a stilbene synthase from *Rheum tataricum*. Phytochemistry 62, 313–323.

Sandur, S.K., Ichikawa, H., Sethi, G., Ahn, K.S., Aggarwal, B.B., 2006. Plumbagin (5-hydroxy-2-methyl-1,4-naphthoquinone) suppresses NF-κB activation and NF-κ-regulated gene products through modulation of p65 and IκBα kinase activation, leading to potentiation of apoptosis induced by cytokine and chemotherapeutic agents. J. Biol. Chem. 281, 17023–17033.

Sankaranarayanan, R., Saxena, P., Marathe, U., Gokhale, R.S., Shanmugam, V.M., Rukmini, R., 2004. A novel tunnel in mycobacterial type III polyketide synthase reveals the structural basis for generating diverse metabolites. Nat. Struct. Mol. Biol. 11, 894–900.

Schmid, H.V., Zenk, M.H., 1971. *p*-Hydroxybenzoic acid and mevalonic acid as precursors of the plant naphthoquinone alkannin. Tetrahedron Lett. 12, 4151–4155.

Schöppner, A., Kindl, H., 1984. Purification and properties of a stilbene synthase from induced cell suspension cultures of peanut. J. Biol. Chem. 259, 6806–6811.

Schröder, J., 2000. The family of chalcone synthase-related proteins: functional diversity and evolution. In: Romeo, J.T., Ibrahim, R.K., Varin, L., De Luca, V. (Eds.), Evolution of Metabolic Pathways, vol. 34. Pergamon Press, Amsterdam, pp. 55–89.

Schröder, J., Raiber, S., Berger, T., Schmidt, A., Schmidt, J., Soares-Sello, A.M., Bardshiri, E., Strack, D., Simpson, T.J., Veit, M., Schröder, G., 1998. Plant polyketide synthases: a chalcone synthase-type enzyme which performs a condensation reaction with methylmalonyl-CoA in the biosynthesis of C-methylated chalcones. Biochemistry 37, 8417–8425.

Schüz, R., Heller, W., Hahlbrock, K., 1983. Substrate specificity of chalcone synthase from *Petroselinum hortense*. Formation of phloroglucinol derivatives from aliphatic substrates. J. Biol. Chem. 258, 6730–6734.

Song, L., Barona-Gomez, F., Corre, C., Xiang, L., Udwary, D.W., Austin, M.B., Noel, J.P., Moore, B.S., Challis, G.L., 2006. Type III polyketide synthase β-ketoacyl-ACP starter unit and ethylmalonyl-CoA extender unit selectivity discovered by *Streptomyces coelicolor* genome mining. J. Am. Chem. Soc. 128, 14754–14755.

Springob, K., Samappito, S., Jindaprasert, A., Schmidt, J., Page, J.E., De-Eknamkul, W., Kutchan, T.M., 2007. A polyketide synthase of *Plumbago indica* that catalyzes the formation of hexaketide pyrones. FEBS J. 274, 406–417.

Sugie, S., Okamoto, K., Rahman, K.M., Tanaka, T., Kawai, K., Yamahara, J., Mori, H., 1998. Inhibitory effects of plumbagin and juglone on azoxymethane-induced intestinal carcinogenesis in rats. Cancer Lett. 127, 177–183.

Tokunaga, T., Dohmura, A., Takada, N., Ueda, M., 2004a. Cytotoxic antifeedant from *Dionaea muscipula* Ellis: a defensive mechanism of carnivorous plants against predators. Bull. Chem. Soc. Jpn. 77, 537–541.

Tokunaga, T., Takada, N., Ueda, M., 2004b. Mechanism of antifeedant activity of plumbagin, a compound concerning the chemical defense in carnivorous plant. Tetrahedron Lett. 45, 7115–7119.

Van de Peer, Y., De Wachter, R., 1994. TREECON for Windows: a software package for the construction and drawing of evolutionary trees for the Microsoft Windows environment. Comput. Appl. Biosci. 10, 569–570.